9.2 RESPONSE OF U.S. WATER RESOURCES TO HADCM2 PROJECTIONS OF CLIMATE CHANGE AND CONSEQUENCES FOR AGRICULTURE

N.J. Rosenberg*, R.C. Izaurralde, R.A. Brown and A.M. Thomson
Joint Global Change Research Institute
Pacific Northwest National Laboratory and the University of Maryland

1. INTRODUCTION

Climate change caused by increasing atmospheric concentrations of greenhouse gases will raise global mean temperatures and have variable impacts on agricultural production in the United States. As agriculture is limited by water supply in many areas, potential changes in the water cycle due to climate change will drive the adaptation of agriculture. The capacity of the atmosphere to hold water increases exponentially with its temperature, increasing evaporation and transpiration rates. Precipitation will also increase as its geographic and temporal patterns change. Although there will be more precipitation overall, not all regions will receive more; some will almost certainly receive less. These expected climatic changes will undoubtedly impact both the supply of and the demand for water. The largest consumptive use of water in the United States is agriculture, the economic sector most likely to be affected by a changing climate. We use climate change scenarios to drive impact assessment models for crop production and water resources. We then link the water resource projections to the crop water demand to identify regions where a change in water supply will most significantly impact crop production.

2. METHODS

Here we report on simulations of agriculture and water resources response to scenarios of climate change derived from the HadCM2 general circulation model (Johns et al., 1997). We examine how the changing supply of water may affect agricultural production and irrigation, one of the more likely ways in which farmers will try to adapt. Baseline climate data from national records for 1961–1990 and the HadCM2 scenario runs for two ten year periods centered on 2030 and 2095 were used to drive the EPIC agricultural and HUMUS hydrological simulation models. HUMUS (Hydrologic Unit Model of the United States; Arnold et al., 1998; Srinivasan et al., 1993), a biophysically based hydrology model, consists of a geographic information system (GIS) that provides data on soils, land use and climate to drive the Soil Water Assessment Tool (SWAT). The hydrology modeling was done at the scale of the 8-digit USGS hydrologic unit area (HUA) (USGS, 1987) of which there are 2101 in the conterminous U.S.

Corresponding author address: N.J. Rosenberg, Joint Global Change Research Institute, 8400 Baltimore Ave. College Park, MD 20740. e-mail:nj.rosenberg@pnl.gov

The variable in HUMUS most comparable to streamflow is 'water yield' which is defined as: runoff + lateral flow + groundwater contribution – transpiration loss – pond abstractions.

EPIC (Erosion Productivity Impact Calculator; Williams, 1995) is a process based agro-ecosystem model used here to simulate corn and alfalfa production with and without irrigation on 204 representative farms across the United States, one representing each USGS 4-digit hydrologic unit area. Both models were run at ambient CO_2 concentrations of 365 and 560 ppm to represent the lack and presence, respectively, of a 'CO_2 fertilization' effect that is known to influence rates of plant photosynthesis and evapotranspiration (ET). The HUMUS results were scaled up from the 8 digit HUA level to the 4 digit HUA level for an analysis of water availability and crop water demand.

3. RESULTS AND DISCUSSION

3.1 *Climate Change Scenarios*

Temperatures increase across the country under the HadCM2 climate change scenarios by up to 4°C for 2030 and 8°C for 2095 (Figure 1). Temperature increases are modest along the East Coast, higher by 1ºC in 2030 and 2.5ºC in 2095, and highest in the Southwest where increases reach 8ºC in 2095. Precipitation also increases over most of the country (Figure 2). The largest increases occur in the Northeast and Pacific Northwest while southern areas see a decrease in 2030, most significantly along the Gulf Coast. The drying trend persists along the Gulf Coast in 2095. The eastern half of the country as well as the West Coast and Mountain regions experience the largest increase in precipitation - over 175 mm above baseline.

HadCM2 projects increased winter precipitation by 2030 across the US except for the Great Lakes and Souris-Red-Rainy basins (Table 1). Reduced summer precipitation is projected for the western US while precipitation increases almost uniformly across the eastern US. HadCM2 predicts substantial increases in winter precipitation in the west by 2095 - 110% in the Great Basin and 40% in the Pacific Northwest. In the Texas Gulf basin, however, winter precipitation decreases by 24%. The trend to greater spring and summer precipitation continues to 2095, except in much of the western US. While almost all of the country is projected to receive more precipitation in all seasons in 2095 as compared with 2030, summer precipitation is actually projected to be lower in the Upper and Lower Colorado and the Great Basin.

3.2 *Water yield*

Consistent with the changing patterns of precipitation, the simulation models project increases in the water supply by 2030 and larger increases in 2095 over most of the country (Figure 3). The exception is the Gulf Coast, where water yield declines. The increases in water yield are greater in magnitude and more widespread geographically in 2095. The higher temperatures also cause rates of ET to rise (Figure 4) and alter seasonal patterns of streamflow in mountainous regions. Regional changes in water supply are variable, with some regions experiencing declines and others increases. In some mountainous regions, the higher temperatures cause a greater proportion of precipitation to fall as rain, thereby reducing the mountain snowpacks and shifting the runoff curve to peak earlier in the spring (Tables 2 and 3). As expected with climate change, potential evapotranspiration increases across the basins, with increases in actual ET under the scenarios presented here. The increases in ET are driven by the greater water availability and are highest in wetter basins. The smallest increase in ET is in the Texas Gulf region where water yields decline significantly in the southern part of the basin (Figure 4).

3.3 *Agriculture*

With more available water, dryland production of corn and alfalfa improves over most of the country. The exception is when the CO_2 fertilization effect is not present - corn yields decline from baseline in western regions while alfalfa yields are less impacted (Table 4). Conditions are projected to be more favorable for irrigated agriculture over much of the country in 2030 and 2095 with the notable exception of the Great Plains.

Simulated irrigated yields of corn generally exceed simulated dryland yields under the baseline climate with no CO_2-fertilization effect. This benefit is evident in the drier portions of the country (southern and northern Plains) and quite substantial in the Pacific and Mountain regions. The advantage accruing to corn irrigation is small in the remainder of the country and even slightly negative in the Delta region. Dryland and irrigated yields of alfalfa are simulated only for five of the ten regions defined by USDA. Under baseline climate with no CO_2-effect alfalfa yields are substantially increased by irrigation in the Pacific and Mountain regions and moderately increased in the Northern and Southern Plains and Corn Belt.

3.4 *Water Supply and Demand*

A proxy indicator was developed using irrigation demand simulated by EPIC and water availability simulated by HUMUS to provide a sense of where in the country, and when, water would be available to satisfy change in irrigation demand for corn and alfalfa production as these are influenced by the HadCM2 scenarios and CO_2-fertilization. Our proxy measure of the relationship between water supply and demand in this study is simple:

$$R_{s/d} = \frac{\Delta(WY - IRR)_{scenario}}{\left|(WY - IRR)_{baseline}\right|}$$

$R_{s/d}$ = Ratio of water supply to irrigation demand
WY = annual water yield from HUMUS
IRR = total irrigation demand of the crop during the growing season

WY is calculated by aggregating water yields simulated by HUMUS at the 8-digit basin scale to the 4-digit scale. IRR is calculated assuming that the crop root zone is fully replenished whenever 50 mm of moisture has been withdrawn from the soil. Thus the amount of irrigation applied is a function of evapotranspiration rate and length of the growing season. WY is an indicator of the volume of water flowing into streams in a particular basin available for withdrawal for irrigation or other uses. The changes in water yield and irrigation demand are presented in Table 5 while the results of the equation are shown in Figures 5 and 6.

In 2030, despite rising temperatures and because of increased rainfall, much of the Eastern Seaboard and New England show up to 50% improvement in water balance (Figure 5). This is true as well of the Pacific Northwest coast with even greater improvement in coastal Northern California, parts of Idaho, Montana and interior Oregon. The remainder of the country, however, shows a general worsening of the water balance, modest in the East and parts of the intermountain West and severe in several 4-digit basins in the Plains region.

Despite still greater increases in temperature in 2095, large increases in precipitation improve water balance over almost all of the eastern U.S. There is a general improvement along the Pacific coast and interior California and in Arizona and the Great Basin. Improvement in water balance occurs in the eastern Great Plains from Minnesota to northern Texas. The simulations reported above support the expectation that suppression of transpiration by elevated CO_2 will increase the availability of water to run off the land or penetrate to depth and will, thereby, increase water yields. Further, the suppression of transpiration in irrigated crops should decrease irrigation requirement. Both effects contribute to an improvement in the supply/demand situation for irrigation water.

4. CONCLUSIONS

Our simulations show an overall increase in water yield nationally. But since regional changes in annual water yield are tightly linked to precipitation patterns, decreases occur in certain regions. Rising temperatures impact annual water yields by increasing ET, thereby reducing quantities of water available for lateral flow and groundwater recharge. Higher temperatures also shift the seasonal hydrologic cycle through earlier snowmelt. This results in a marked increase in water yield during late winter and early spring and in some cases a reduction in water supply during summer. This effect is most evident in the western basins whose hydrologic systems are dominated by snowmelt. Additionally, seasonal shifts in the annual hydrograph are most pronounced under the warmer and wetter HadCM2 scenario for 2095. Conditions are projected to be more favorable for irrigated agriculture over much of the country in 2030 and 2095. A notable exception is the Great Plains, a major agricultural region, where irrigation demands may not be met by available water supply under climate change.

5. REFERENCES

Arnold, J.G., Srinivasan, R., Muttiah, R.S., Williams, J.R., 1998. Large area hydrologic modeling and assessment, Part I: model development. J. Amer. Wat. Res. Assc. 34, 1-17.

Johns, T.C., Carnell, R.E., Crossley, J.F., Gregory, J.M., Mitchell, J.F.B., Senior, C.A., Tett, S.F.B., Wood, R.A., 1997. The Second Hadley Centre coupled ocean-atmosphere GCM: Model description, spinup and validation. Climate Dynamics 13, 103-134.

Srinivasan, R., J.G. Arnold, R.S. Muttiah, C. Walker and P.T. Dyke, 1993. Hydrologic Unit Model for the United States (HUMUS). In Advances in Hydroscience and Engineering. CCHE, School of Engineering, University of Mississippi, Oxford, MS.

USGS, 1987. Hydrologic Unit Maps. Rep. No. 2294, US Government Printing Office, Washington, DC.

Williams, J.R., 1995. The EPIC model. In: Singh, V.P. (Ed.), Computer Models of Watershed Hydrology, Water Resources Public. Highlands Ranch, CO, p. 909–1000.

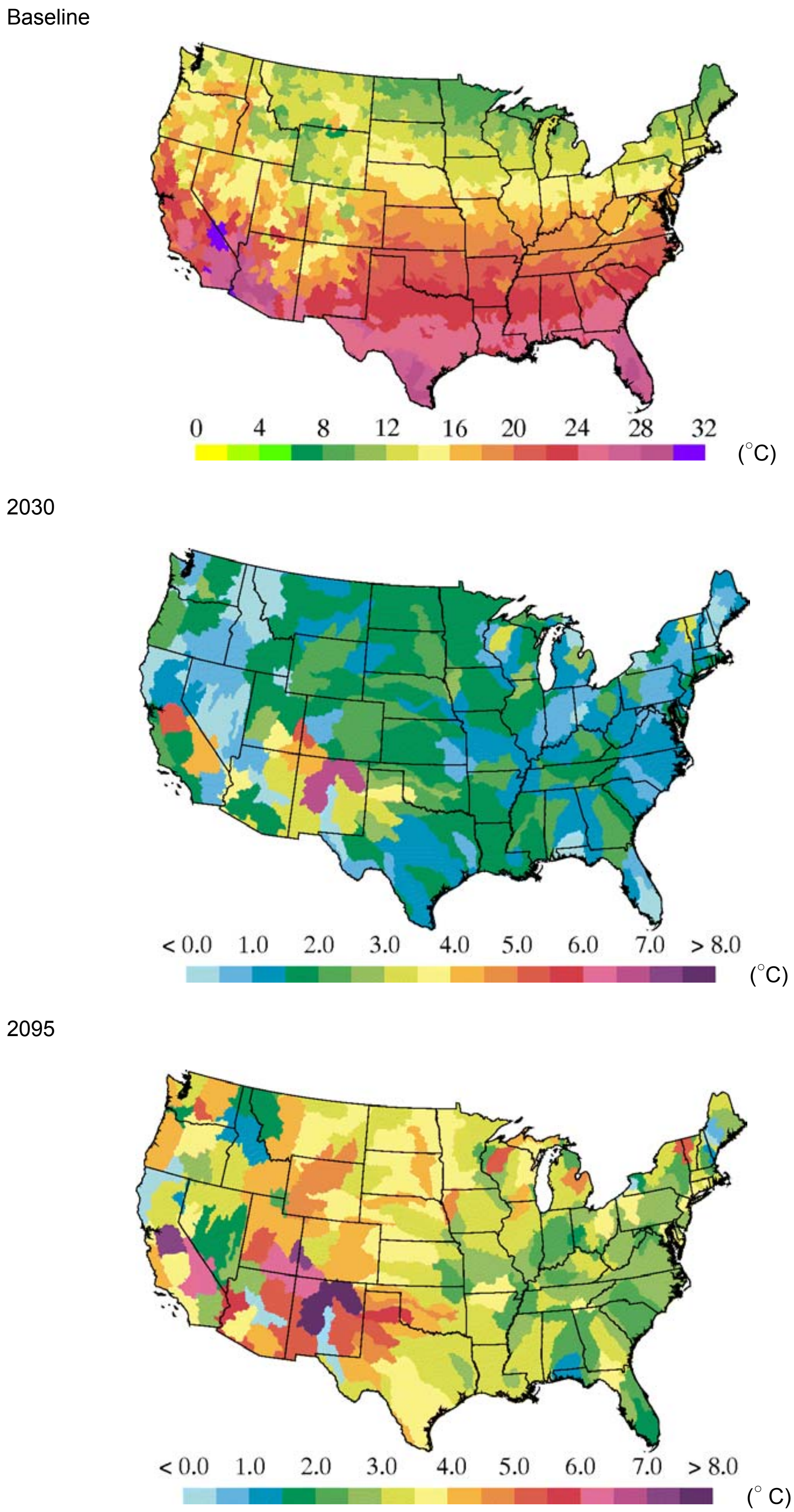

Figure 1. Temperature at baseline and change under 2 HADCM2 scenarios.

Baseline

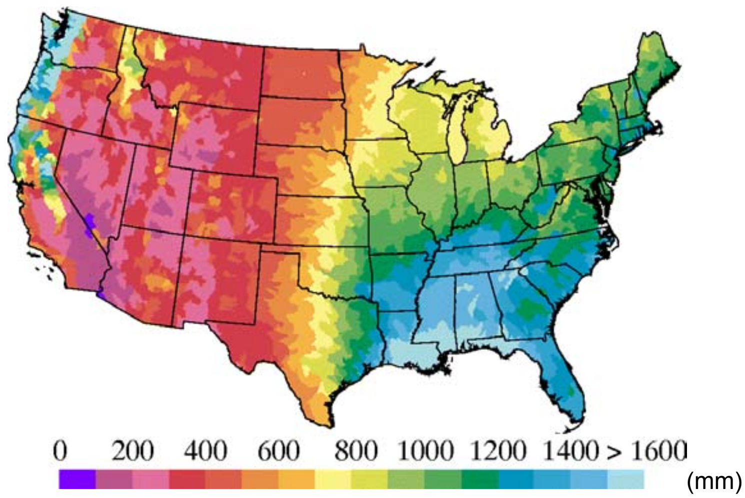

2030

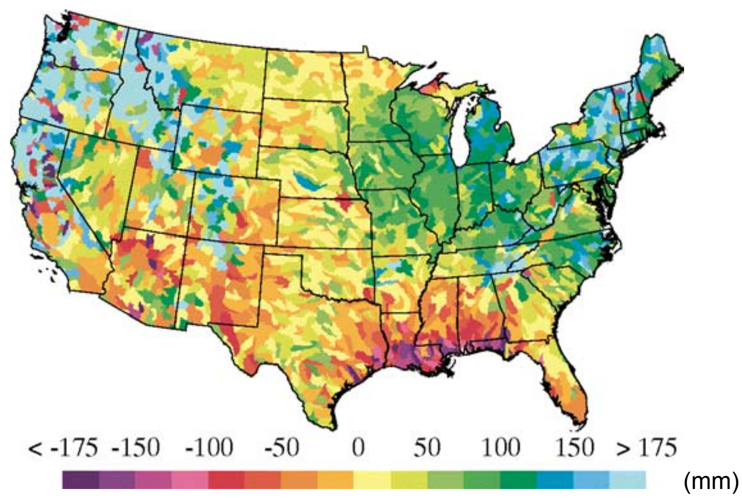

2095

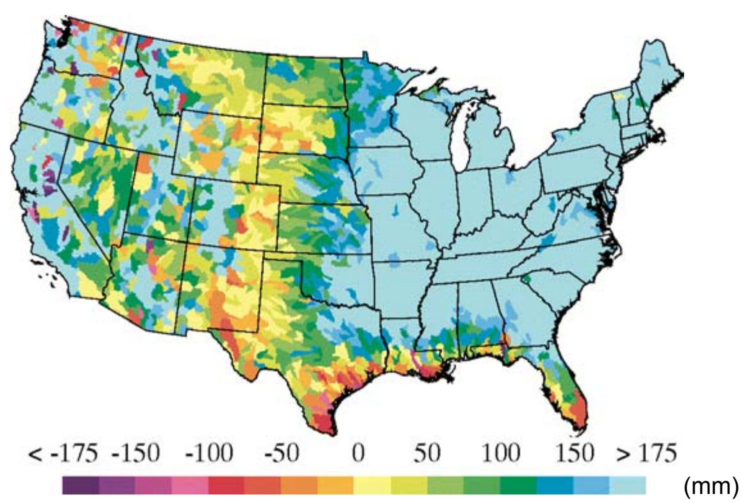

Figure 2. Precipitation at baseline and under two HADCM2 scenarios.

Table 1. Seasonal mean precipitation totals aggregated from the 8-digit HUAs to the MWRR level for baseline climate and percentage deviations from baseline for the HadCM2 scenarios of 2030 and 2095 by MWRR.

	DJF			**MAM**			JJA			SON		
MWRR	Baseline	2030	2095	Baseline	2030	2095	Baseline	2030	2095	Baseline	2030	2095
	mm	----------% ----------		mm	----------% ----------		mm	----------% ----------		mm	----------% -------	
1 (NE)	246	10	41	263	5	7	284	23	33	289	8	25
2 (MA)	218	9	30	267	9	21	295	17	28	263	5	25
3 (SAG)	323	5	8	333	-8	10	408	-6	18	275	16	23
4 (GL)	143	-4	26	204	10	10	257	24	45	235	14	39
5 (OH)	232	13	14	312	11	28	309	8	32	252	2	32
6 (TN)	348	17	11	382	1	25	323	4	48	298	10	36
7 (UMS)	100	2	16	230	11	22	297	12	31	214	9	32
8 (LMS)	365	4	-3	389	-5	15	327	-13	26	318	3	28
9 (SRR)	46	-13	18	127	-4	10	237	10	16	121	-4	42
10 (MO)	48	13	35	156	14	23	190	5	4	108	5	25
11 (ARK)	112	15	16	226	-1	24	233	-4	17	198	4	19
12 (TG)	146	4	-24	207	-2	4	212	1	24	235	-5	12
13 (RG)	45	56	37	55	19	24	141	-11	0	106	-15	11
14 (UCO)	61	45	92	71	37	52	78	-6	-12	81	7	60
15 (LCO)	79	67	82	50	4	76	98	-39	-37	80	-31	41
16 (GB)	65	39	110	74	39	58	58	-16	-26	67	21	58
17 (PNW)	255	25	40	160	33	37	85	16	6	177	59	44
18 (CA)	259	16	68	130	36	54	22	-1	17	127	7	35

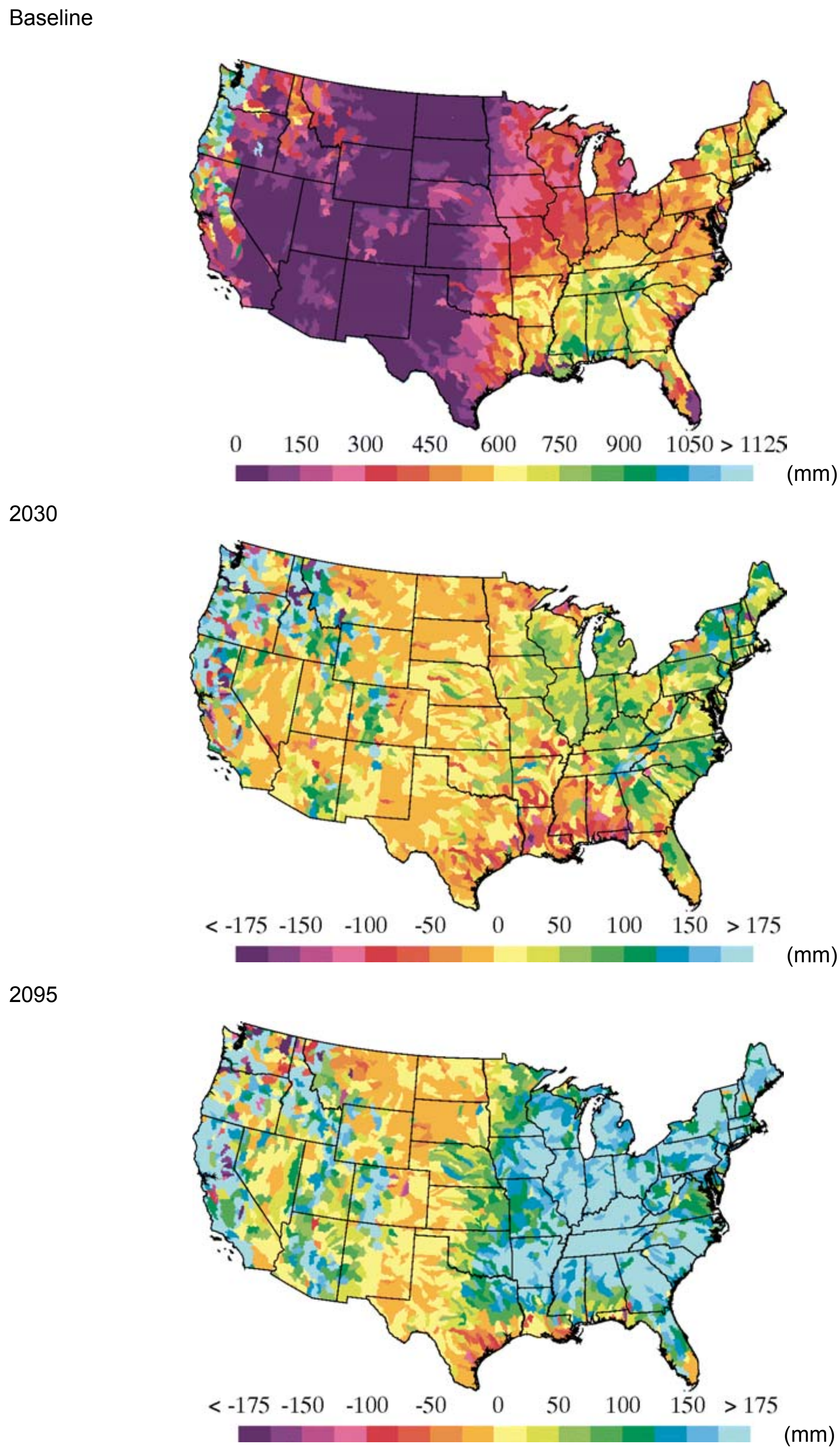

Figure 3. Water Yield simulated at baseline and change under climate change

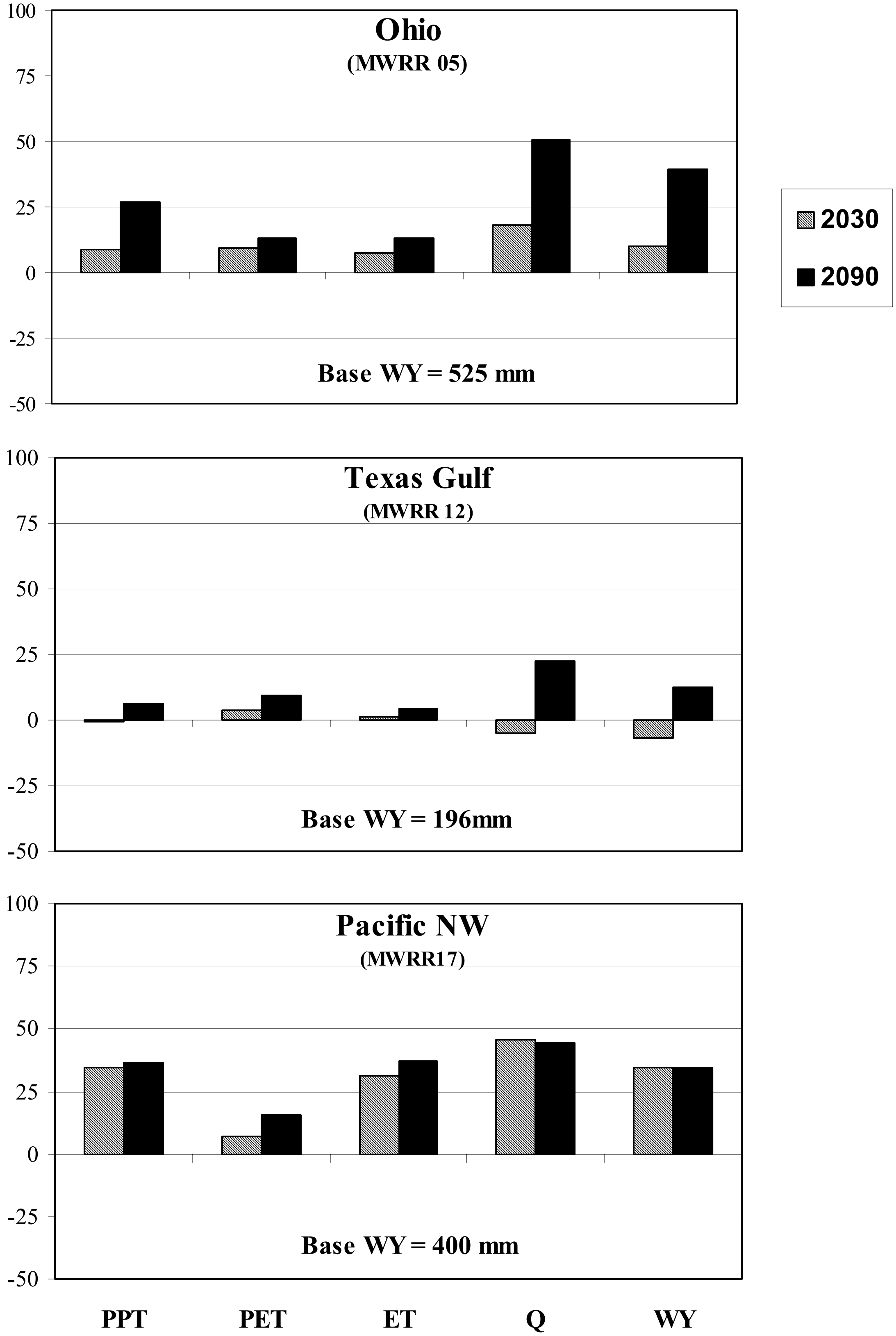

Figure 4. Percentage change in water supply and use variables for selected MWRRs.

Table 2. Simulated evapotranspiration (ET), potential evapotranspiration (PET), surface runoff (Q) and water yield (WY) for the major water resource regions under baseline climate and under climate change in 2030 projected by the HadCM2 model, with and without ‘CO_2-fertilization’

Scenario	Baseline			Baseline			Baseline			Baseline		
CO_2 (ppm)	365	365	560	365	365	560	365	365	560	365	365	560
	ET	Δ ET		PET	Δ PET		Q	Δ Q		WY	Δ WY	
MWRR	*mm*											
1 (NE)	399	45	13	804	101	87	360	45	61	598	62	90
2 (MA)	425	36	16	982	94	92	275	51	60	520	60	75
3 (SAG)	564	-2	-34	1313	91	82	279	37	47	607	18	41
4 (GL)	498	40	26	989	62	60	199	25	32	330	32	45
5 (OH)	539	41	22	1080	104	104	358	66	76	525	53	69
6 (TN)	543	23	-2	1085	86	84	315	69	76	759	82	104
7 (UMS)	512	41	26	1076	115	114	237	40	51	313	35	50
8 (LMS)	656	12	-27	1271	111	102	373	-5	14	586	-31	2
9 (SRR)	449	24	17	1130	130	128	62	-18	-13	82	-19	-11
10 (MO)	406	34	27	1306	155	154	68	5	10	94	8	14
11 (ARK)	544	9	-6	1700	139	136	150	11	21	211	5	19
12 (TG)	577	9	-9	1881	71	67	121	-6	4	196	-14	3
13 (RG)	318	-3	-6	1731	158	158	10	4	5	29	5	7
14 (UCO)	237	20	17	1215	112	109	25	13	13	53	32	34
15 (LCO)	260	-29	-30	1748	138	136	12	11	11	46	18	19
16 (GB)	217	34	32	1308	125	125	28	7	8	48	23	25
17 (PNW)	235	74	60	1000	70	44	192	87	92	400	139	153
18 (CA)	217	29	24	1394	44	41	119	29	31	290	54	59

Table 3. Simulated evapotranspiration (ET), potential evapotranspiration (PET), surface runoff (Q) and water yield (WY) for the major water resource regions under baseline climate and under climate change in 2095 projected by the HadCM2 model, with and without ‘CO_2-fertilization’

Scenario	Baseline			Baseline			Baseline			Baseline		
CO_2(ppm)	365	365	560	365	365	560	365	365	560	365	365	560
	ET	Δ ET		PET	Δ PET		Q	Δ Q		WY	Δ WY	
MWRR	----------mm----------											
1 (NE)	399	66	32	804	158	145	360	117	134	598	185	214
2 (MA)	425	56	36	982	147	144	275	119	127	520	168	183
3 (SAG)	564	23	-9	1313	136	128	279	118	128	607	149	172
4 (GL)	498	65	52	989	112	110	199	83	90	330	138	151
5 (OH)	539	70	53	1080	144	143	358	181	190	525	206	220
6 (TN)	543	55	33	1085	115	114	315	199	206	759	321	342
7 (UMS)	512	68	54	1076	162	161	237	127	138	313	151	166
8 (LMS)	656	54	14	1271	156	142	373	133	153	586	149	183
9 (SRR)	449	76	66	1130	182	180	62	9	15	82	22	31
10 (MO)	406	55	48	1306	240	239	68	24	29	94	31	37
11 (ARK)	544	56	38	1700	214	211	150	77	88	211	87	103
12 (TG)	577	24	4	1881	172	167	121	27	39	196	25	44
13 (RG)	318	10	7	1731	265	264	10	12	13	29	25	28
14 (UCO)	237	41	37	1215	210	206	25	32	33	53	83	86
15 (LCO)	260	9	7	1748	225	224	12	34	34	46	81	83
16 (GB)	217	62	60	1308	219	219	28	28	30	48	70	73
17 (PNW)	235	87	74	1000	157	144	192	85	89	400	138	149
18 (CA)	217	62	55	1394	125	122	119	98	100	290	199	204

Table 4. Simulated yields of corn and alfalfa under baseline climate (B) and the HadCM2 projections in 2030 (H1) and 2095 (H2), each at two CO_2 concentration levels (365 and 560 ppm) under dryland and irrigated conditions.

CO_2 / Scenario	Region: Pacific		Mountain		N. Plains		S. Plains		Lakes		Corn Belt		Delta		Northeast		Appalachian		Southeast	
	---Mg ha^{-1}---																			
Dryland Corn																				
B-365	1.38	a	0.98	bc	4.6	ba	5.55	b	4.57	d	6.05	c	6.26	ba	4.16	d	6.13	bc	5.76	ba
H1-365	1.08	a	0.51	d	3.11	d	4.33	c	5.3	c	6.31	cb	5.84	b	4.7	bdc	5.94	c	5.34	ba
H1-560	1.42	a	0.8	dc	4.2	bc	5.7	ba	5.94	b	6.98	a	6.74	a	5.24	ba	6.7	ba	6.13	ba
H2-365	1.71	a	0.76	dc	3.48	dc	4.2	c	6.04	b	6.53	b	5.84	b	4.81	bac	6.27	bac	5.04	b
H2-560	2.15	a	1.18	ba	4.51	b	5.23	bc	6.69	a	7.09	a	6.32	ba	5.35	a	6.95	a	5.76	ba
Irrigated Corn																				
B-365	5.39	b	4.47	c	5.66	d	7.7	bc	4.65	d	6.15	c	6.14	b	4.24	c	6.32	b	5.8	a
H1-365	5.53	ba	5.53	b	6.52	b	7.81	bc	5.82	c	6.69	b	6.84	ba	5.02	ba	6.57	ba	5.82	a
H1-560	6.01	ba	6	ba	7.02	a	8.41	a	6.24	cb	7.2	a	7.28	a	5.44	a	7.17	a	6.48	a
H2-365	6.48	ba	5.67	ba	6.24	c	6.72	d	6.42	b	6.68	b	6.03	b	5.08	ba	6.52	ba	5.42	a
H2-560	7.02	a	6.17	a	6.72	b	7.27	dc	6.89	a	7.17	a	6.38	ba	5.5	a	7.11	ba	6.06	a
Dryland Alfalfa																				
B-365	4.34	b	3.08	c	5.57	bc	6.85	c			7.66	c								
H1-365	4.51	ba	3.09	c	4.68	c	7.76	b			8.64	b								
H1-560	5.81	ba	4.05	ba	6.16	ba	9.53	a			10.44	a								
H2-365	5.15	ba	3.6	bc	5.17	c	8.27	b			9.23	b								
H2-560	6.68	a	4.69	a	6.81	a	10.03	a			10.97	a								
Irrigated Alfalfa																				
B-365	10.7	d	9.21	c	7.71	c	7.17	d			7.99	c								
H1-365	11.92	dc	10.9	b	9.35	b	9.07	cb			9.58	b								
H1-560	14.08	ba	12.8	a	10.98	a	10.59	a			11.17	a								
H2-365	12.11	dc	10.94	b	9.69	b	9.23	b			9.72	b								
H2-560	14.37	a	12.87	a	11.41	a	10.77	a			11.31	a								

† Means within a column and section followed by the same letter are not significantly different at the 10% level of probability.

Table 5. Water yield and irrigation requirement (mm) for corn and alfalfa under baseline, climate change, and CO_2-fertilization scenarios

Scenario		Baseline		HadCM2 2030				HadCM2 2095			
Variable		Water Yield	Irrigation	Δ Water Yield		Δ Irrigation		Δ Water Yield		Δ Irrigation	
CO_2 (ppm)				365	560	365	560	365	560	365	560
MWRR	HUA 4					Corn					
New Eng.	107	584	46	42	56	54	31	139	154	57	37
Mid-Atl.	205	518	69	74	89	61	17	196	211	54	19
S.Atl.-Gulf	305	526	13	39	55	50	31	187	204	17	11
Great Lakes	408	302	107	61	74	74	31	160	173	85	46
Ohio	512	455	102	63	78	87	46	211	226	57	13
Tenn.	603	804	111	55	72	154	115	310	328	67	30
U. Miss.	708	296	80	51	65	106	63	186	199	78	41
L. Miss.	805	604	52	-8	4	235	174	198	212	107	44
Souris-R.-R	902	56	102	-18	-13	133	85	13	21	119	69
Missouri	1012	33	206	-9	-7	119	52	-10	-9	104	37
Ark-W.-R.	1103	81	228	8	14	144	72	25	33	98	33
TX Gulf	1209	151	300	-2	10	119	61	17	32	98	22
Rio Grande	1306	18	278	-11	-11	237	146	-2	0	237	159
U. Colorado	1406	29	313	9	11	183	109	50	53	163	91
L. Colorado	1507	32	593	18	20	-7	-96	89	90	-81	-148
Great Basin	1604	42	492	22	23	67	-17	42	43	31	-51
Pacific NW	1702	186	380	106	112	174	70	54	59	163	70
California	1804	398	267	21	23	406	304	150	153	352	258
MWRR	HUA 4					Alfalfa					
Great Lakes	408	302	181	61	74	133	59	160	173	148	70
Ohio	512	455	154	63	78	94	37	211	226	83	26
U. Miss.	708	296	154	51	65	196	143	186	199	163	74
Souris-R.-R.	902	56	204	-18	-13	313	228	13	21	319	226
Missouri	1012	33	289	-9	-7	226	150	-10	-9	300	206
Ark.-W.-R.	1103	81	578	8	14	407	250	25	33	433	294
Rio Grande	1306	18	804	-11	-11	550	367	-2	0	719	528
U. Colorado	1406	29	567	9	11	280	178	50	53	341	222
L. Colorado	1507	32	1613	18	20	185	0	89	90	19	-181
Great Basin	1604	42	759	22	23	113	-22	42	43	261	106
Pacific NW	1702	186	622	106	112	393	246	54	59	531	369
California	1804	398	498	21	23	361	252	150	153	431	31

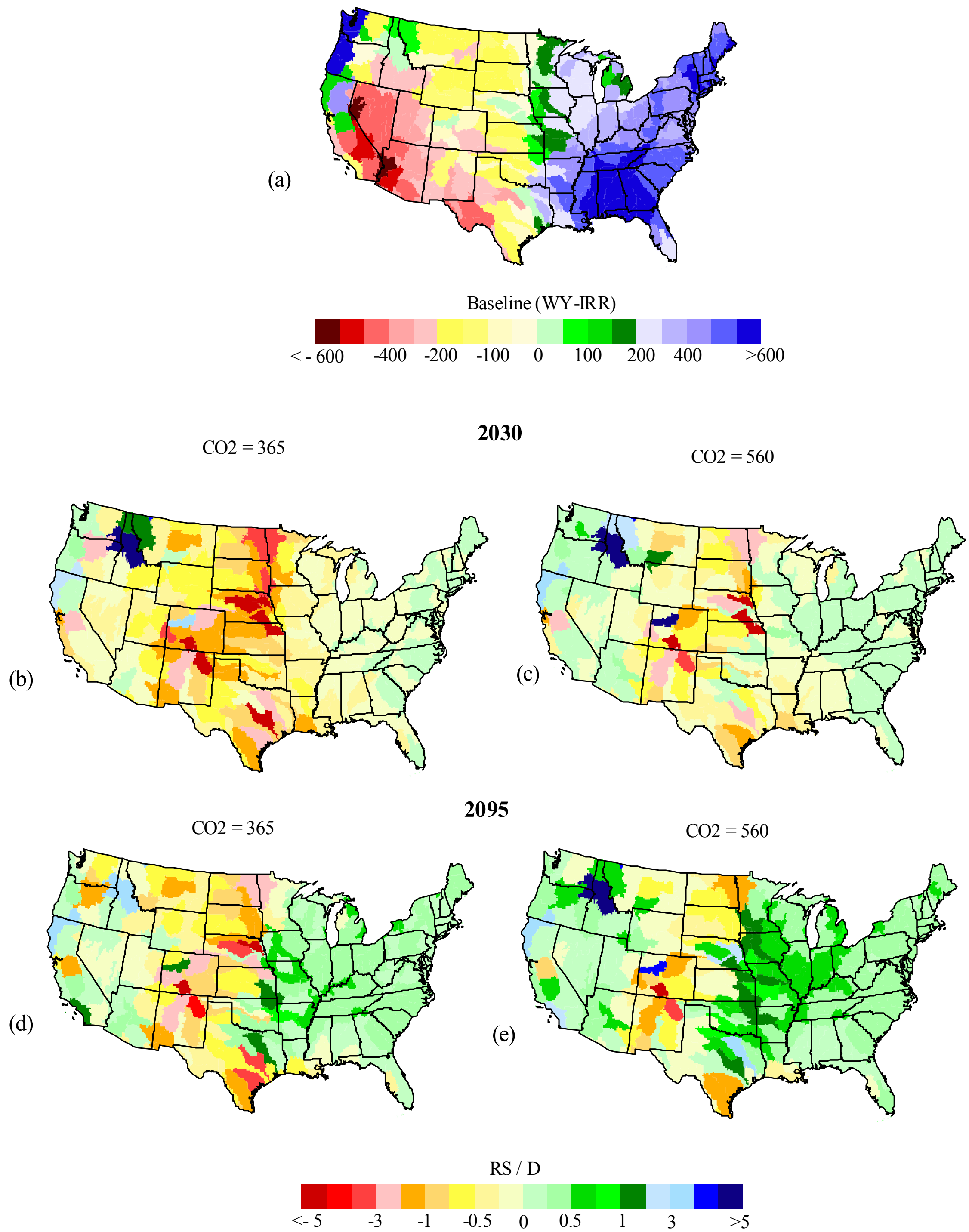

Figure 5. Difference in water supply and demand simulated with the HUMUS and EPIC models, respectively, under baseline climate conditions for irrigated corn

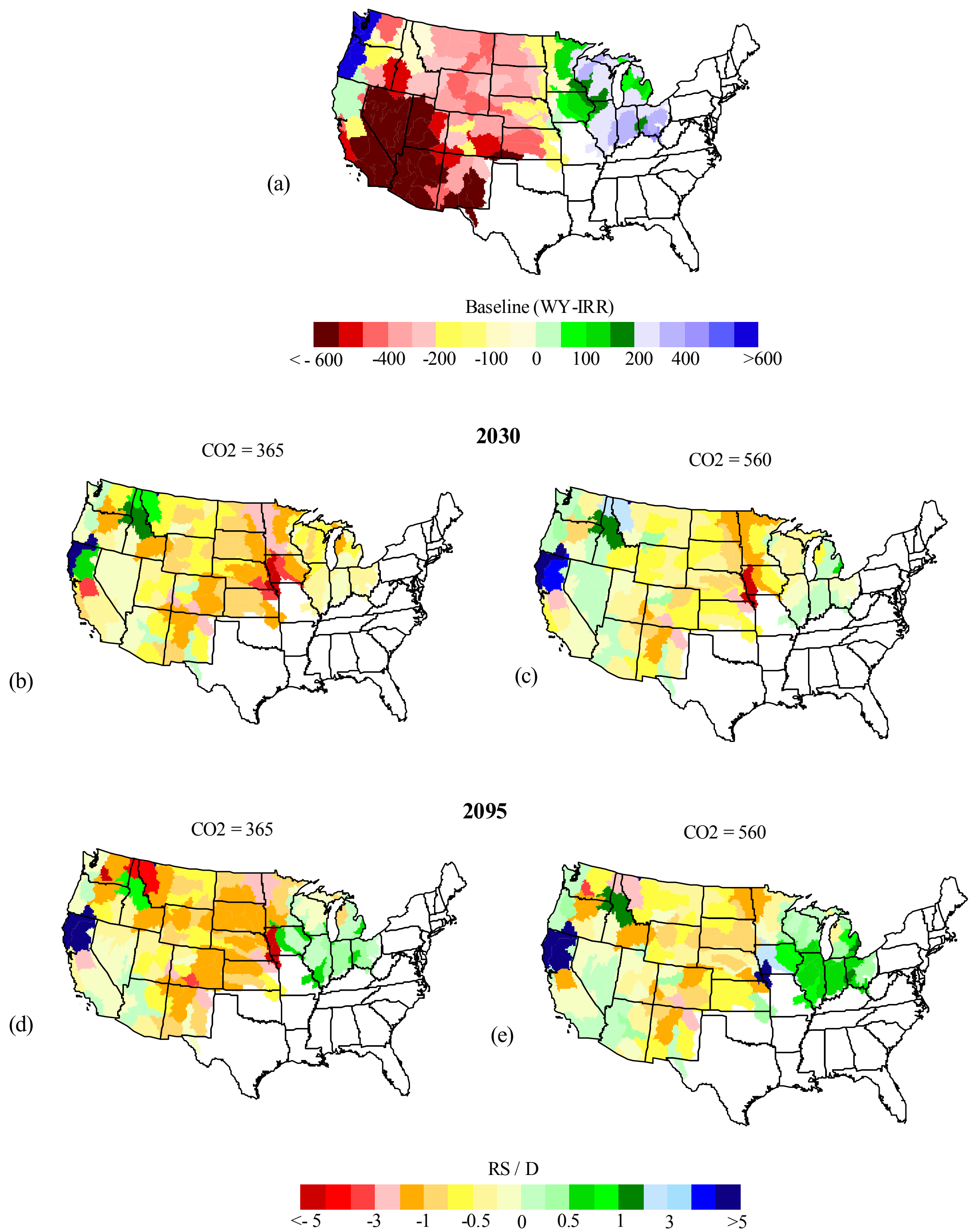

Figure 6. Difference in water supply and demand simulated with the HUMUS and EPIC models, respectively, under baseline climate conditions for irrigated alfalfa